

V. S. TINKOVA<sup>1</sup>, A. G. YAKUBOVSKAYA<sup>1</sup>, I. A. TUPITSYNA<sup>1</sup>, S. L. ABASHIN<sup>2</sup>,  
A. N. PUZAN<sup>3</sup>, S. O. TRETYAK<sup>1</sup>

Ukraine, Kharkov, <sup>1</sup>Institute for Scintillation Materials NAS of Ukraine;

<sup>2</sup>National Aerospace University "Kharkiv Aviation Institute";

<sup>3</sup>SSI "Institute for Single Crystals" NAS of Ukraine

E-mail: zvereva@isma.kharkov.ua

## FLEXIBLE COMPOSITE SCINTILLATORS BASED ON ZnWO<sub>4</sub> MICRO- AND NANOPOWDERS

*Nano-sized and micro-sized ZnWO<sub>4</sub> powders were obtained by different methods: hydrothermal synthesis with microwave heating, molten salt method, solid-state synthesis and crushing of bulk crystals. Their morphological features were studied using transmission electron microscope and scanning electron microscope. The obtained nano- and micro-sized powders were used as fillers for flexible composite scintillators. The silicon rubber was used as a binder. The luminescent characteristics and scintillation performance of composite scintillators were measured. The dependence of scintillation performance of flexible scintillators on the morphological features of ZnWO<sub>4</sub> nanocrystallites was demonstrated. The flexible composite scintillator based on zinc tungstate obtained by solid-state synthesis with lithium nitrate addition was obtained and investigated. Its scintillation performance was close to that of a ZnWO<sub>4</sub> single crystal.*

*Keywords: zinc tungstate, nano-sized crystals, micro-sized powders, composite scintillators, light output, afterglow.*

There is now an ongoing research of effective technological methods for obtaining materials suitable for use in modern scintillation detectors (for nondestructive testing, digital radiography and X-ray,  $\alpha$ ,  $\beta$ ,  $\gamma$  and neutron registration). The creation of composite scintillators based on micro- and nanoscale crystal powders [1] obtained by various methods [2–4] is a promising research direction in this field.

It was expected that using nano-sized materials would allow developing qualitatively new scintillators with functional characteristics that would satisfy the modern requirements (spatial, spectrometric and temporal resolution, sensitivity, radiation hardness, low afterglow) [5, 6]. The properties of nano-sized scintillation powders significantly depend on their size and morphology, and controlling this parameters allows producing scintillation detectors with high performance [7].

Zinc tungstate (ZnWO<sub>4</sub>) is a promising material that could be a successful replacement for cadmium tungstate which contains toxic cadmium. It is possible because ZnWO<sub>4</sub> has the unique combination of properties (high density, high effective atomic number, small radiation length and scintillation performance) similar to those of cadmium tungstate. Therefore, ZnWO<sub>4</sub> can be used in X-ray, gamma and neutron radiation

detectors in homeland security systems and for non-destructive testing.

Thus, the primary task of the work was to choose the best method to produce ZnWO<sub>4</sub> powder for development of high performance flexible composite scintillators.

### Research methodology

ZnWO<sub>4</sub> single crystals grown by Czochralski method [8] were used to obtain powders with different grains sizes. The crushing of ZnWO<sub>4</sub> single crystals was carried out with laboratory mechanical mortar Retch RM 200. The following fractionation was carried out with vibratory sieve shaker Retch AS 200 using sieves No 0080, 0100, 0140, 0200, 0250.

For the preparation of 0.1 M aqueous solutions Zn(NO<sub>3</sub>)<sub>2</sub>·6H<sub>2</sub>O (99.9%) and Na<sub>2</sub>WO<sub>4</sub>·2H<sub>2</sub>O (>99.9%) were used. Before the synthesis the solutions were mixed with a ratio of 1:1. The pH of the mixture was changed by addition of 30% NH<sub>3</sub>·H<sub>2</sub>O solution (99%). ZnWO<sub>4</sub> powder was synthesized from the obtained mixture by microwave-hydrothermal method.

ZnO (99.995%) and WO<sub>3</sub> (99.995%) were used as starting materials for the synthesis of ZnWO<sub>4</sub> scintillation powder by molten salt and solid-state methods. LiNO<sub>3</sub>·6H<sub>2</sub>O (99.9%) was used as a low-temperature solvent and as a mineralizer in molten salt and solid-state methods, respectively.

Morphology of the nano-sized crystals was determined using transmission electron microscope

This work was supported by National Academy of Science of Ukraine through grant of young scientists' project of NAS of Ukraine in 2017, contract No. 51-2017.

(TEM) EM-125 (SELMA, Ukraine). Electron accelerating voltage was 125 keV, the survey was carried out in the bright field mode, and the image was recorded by CCD matrix. The carbon films coated with water suspension of the investigated powders were used for electron microscopy.

Morphology of the micro-sized crystals was determined using scanning electron microscope (SEM) REM-100U with energy dispersive attachment EDAR.

X-ray diffraction study (XRD) was carried out using Siemens D500 automated powder diffractometer ( $\text{Cu}_{K\alpha}$  radiation, Ni filter,  $5^\circ \leq 2\theta \leq 110^\circ$ ,  $\Delta 2\theta = 0.02^\circ$ , delay time of 24 s per point). Rietveld refinement of obtained pattern was carried out with FullProf and WinPLOTR software packages [9]. Cell dimensions, anisotropic profile function, background function and systematic instrumental errors were taken into account.

Flexible scintillation composite samples ( $\varnothing 30 \times 2$  mm) based on  $\text{ZnWO}_4$  powders obtained by different methods were prepared. The heat-resistant low molecular silicone rubber was used as a binder. The luminescent and scintillation characteristics of the composite samples were investigated.  $\text{ZnWO}_4$  and  $\text{CdWO}_4$  polished plates with size of  $10 \times 10 \times 2$  mm were used as references during the measurements of scintillation performances. Both reference plates were cut from crystals grown by Czochralski method. The light yield of  $\text{CdWO}_4$  was measured in [10] as 19500 ph/MeV.

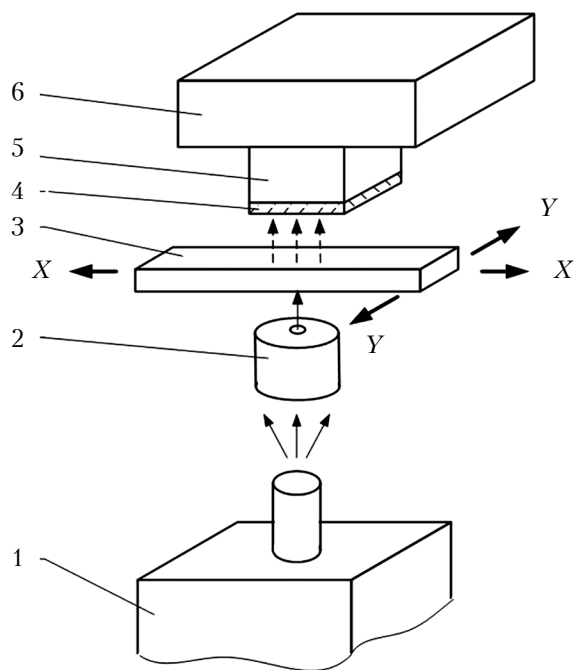


Fig. 1. Scheme of light output measurements:

1 – X-ray source; 2 – collimator; 3 – objective table; 4 – protective filter; 5 – photodetector; 6 – amplifier

X-ray luminescence spectra were measured by spectrometric complex KSVU-23. REIS ( $U_\alpha \leq 40$  keV,  $I_\alpha \leq 50$   $\mu\text{A}$ ) X-ray source was used for excitation.

Light output of the investigated composite samples was measured in scanning mode with respect to  $\text{ZnWO}_4$  and  $\text{CdWO}_4$  single crystals by the scheme which is presented in Fig. 1. The objective table 3 with investigated samples moves between the photodetector 5 and X-ray tube (focal spot 0.8 mm) in a plane XY with a step of 3 mm, which can be changed in manual mode. X-ray transmission optical scheme was used during measurements. The different light collection conditions were considered. X-ray source ( $U_\alpha = 100$  keV,  $I_\alpha = 1$  mA) was used for excitation. The measurement error of the light output was 12%.

The afterglow level was determined by means of a measuring set up which included a pulsed X-ray source RAPAN 200/100 ( $U_\alpha = 130 - 180$  kV, irradiation time 2 s), a control unit, a Si-photodiode S8594, a current-to-voltage converter, a multiplexer, an analog-to-digital converter, and a computer with an appropriate software. The measurement error of the afterglow level was 10%.

### Experimental results and discussion

#### *Flexible composite scintillators based on $\text{ZnWO}_4$ obtained by crushing of bulk crystals*

Micro- and nanocrystallites  $\text{ZnWO}_4$  used as fillers for composite scintillators were obtained by crushing of bulk crystals [11]. The advantages of the method are the high speed of the process and the simplicity of the milling hardware. The feature of the method is wide particles size distribution of resulting crystallites (from several nanometers to hundreds of micrometers).

As a result of  $\text{ZnWO}_4$  single crystal crushing we obtained the following ratio of the particle size fractions: more than  $280 \mu\text{m}$  was 4.5%;  $140 - 280 \mu\text{m}$  was 33.5%;  $80 - 140 \mu\text{m}$  was 26%, less than  $80 \mu\text{m}$  was 36% [12]. The composite sample (further denoted as ZWO-30) based on as-crushed crystal was prepared. During the polymerization of the binder the sedimentation of  $\text{ZnWO}_4$  particles takes place. Large particles settle on the bottom of the mold for casting, while particles of several tens of nanometers remain in suspension forming a dense composite surface. SEM-evaluation of the composite scintillator surfaces has shown that  $\text{ZnWO}_4$  particles about 250 nm in size were located on the top side and particles with average size of  $250 \mu\text{m}$  were on the bottom side of the composite sample. (Further these surfaces will be denoted as ZWO-30-250nm and ZWO-30-250 $\mu\text{m}$ , respectively.)

The light output of the obtained samples was determined by two methods, i. e. the light output

was estimated by cathodoluminescence technique and measured under X-ray excitation.

The technique for measuring light output under cathode excitation is described in [11]. It should be noted that the experimental conditions of light output estimation used in [11] have minimized the influence of light collection due to reflection-type optical scheme in the measurements of cathodoluminescence intensity.

The light output was determined for the both sides of the sample (ZWO-30-250nm and ZWO-30-250μm) based on the cathodoluminescence results. The penetration depth of the high-energy electron beam into the surface was very small and only luminescence of the surface layers was observed under irradiation. The light output of the ZWO-30-250nm (97 a. u.) was almost twice higher than that of the ZWO-30-250μm (45 a. u.) and the ZnWO<sub>4</sub> single crystal (46 a. u.) [11].

The light output of the ZWO-30 under X-ray excitation was determined using the optical transmission scheme shown in Fig. 1. The light output of the ZWO-30 under X-ray excitation was measured from both top and bottom sides (Table 1). The ZWO-30 sample and ZnWO<sub>4</sub> single crystal reference were placed on a white diffuse reflector. The relative light outputs of ZWO-30-250μm and ZWO-30-250nm were 280% and 227% of ZnWO<sub>4</sub> single crystal, respectively. It could be due to size gradient distribution of particles through the thickness of the composite samples (as a consequence of the sedimentation described above) [12]. As a result, the best light collection conditions for this measurement method were achieved on ZWO-30-250μm. Further in the article it will be shown that the change of light collection condi-

tions shows significant effect on the light output of composite scintillators.

The measurement results demonstrate that the described preparation method of scintillation powder allows obtaining composite scintillators based on ZnWO<sub>4</sub> with high scintillation performance. However, mass production of such composite scintillators is expensive. Therefore, it is desirable to find ways of preparing ZnWO<sub>4</sub> powder with good scintillation characteristics by passing the growth stage and the following crushing of a single crystal.

*Flexible composite scintillators based on ZnWO<sub>4</sub> obtained by hydrothermal synthesis with microwave heating*

Hydrothermal synthesis with microwave heating allows controlling all parameters of the reaction (time, temperature, pressure), which ensures homogeneous nucleation process under homogeneous heating of the reaction mixture and yields in dispersion of high purity with a specified narrow particle size distribution [13]. The method also allows obtaining specified morphology of nanocrystals, which directly relates to the electronic structure, binding energy and surface energy [14].

The hydrothermal synthesis of zinc tungstate nanocrystals was carried out using microwave heating of aqueous solutions of Zn(NO<sub>3</sub>)<sub>2</sub>·6H<sub>2</sub>O and Na<sub>2</sub>WO<sub>4</sub>·2H<sub>2</sub>O (pH = 6.5–9.5) at temperatures of 120–200°C for 30 min [14]. The results of XRD (Fig. 2) showed that the nucleation of ZnWO<sub>4</sub> nanocrystals with a monoclinic wolframite structure (JCDPS No 15-0774 [15]) begins at 120°C. The increase in temperature and pH accelerates the growth of the crystallites.

The investigation of ZnWO<sub>4</sub> nanopowders morphology using TEM showed that samples synthesized at pH = 9.5 and temperature of 120°C, consisted of “grain” nanoparticles with a size of 25–50 nm, while those synthesized at 200°C

Table 1

*The light output under X-ray excitation of composite scintillators based on ZnWO<sub>4</sub> obtained by different methods*

Method	Sample	Light output, %
Czochralski	Polished ZnWO <sub>4</sub> single crystal	100
Crushed crystal	ZWO-30-250μm	280
	ZWO-30-250nm	227
Hydrothermal synthesis with microwave heating	ZWO-25g	16
	ZWO-100r	23
	ZWO-200r	30
Molten salt synthesis	ZWO-MSM	67
Solid-state synthesis	ZWO-SSS	155
	ZWO-SSS-LiNO <sub>3</sub>	272

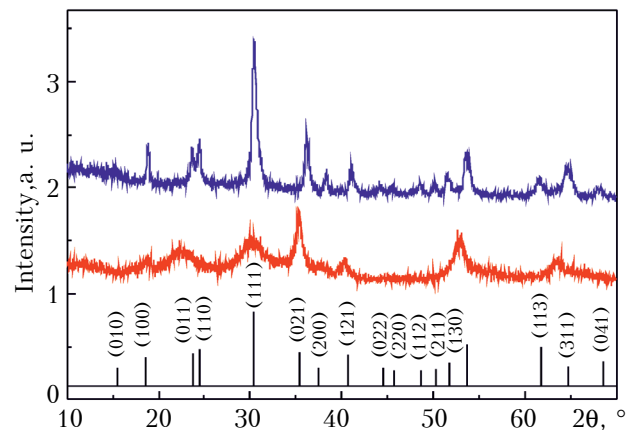


Fig. 2. X-ray diffraction patterns of ZnWO<sub>4</sub> nanocrystals obtained by hydrothermal synthesis with microwave heating at pH = 9.5 and different temperature values

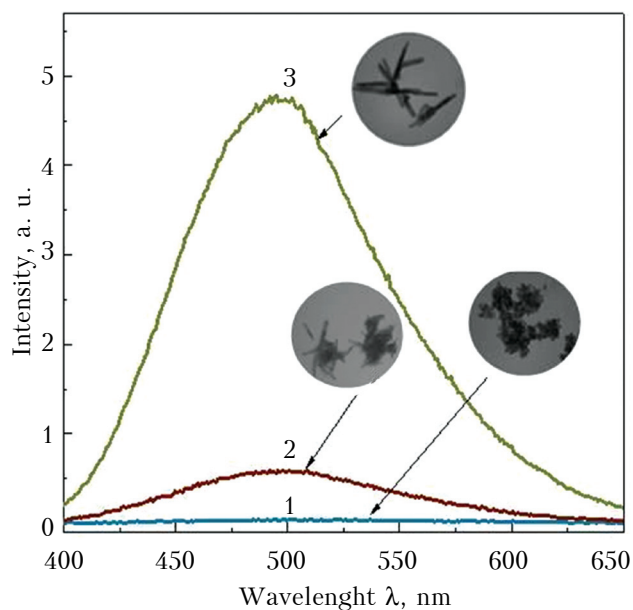


Fig. 3. X-ray luminescence spectra of  $\text{ZnWO}_4$  nanopowders obtained by hydrothermal synthesis with microwave heating at  $\text{pH} = 9.5$  and different temperature values:  
1 –  $120^\circ\text{C}$ ; 2 –  $160^\circ\text{C}$ ; 3 –  $200^\circ\text{C}$

consisted of “rod” nanoparticles of 250–300 nm in length and 30 nm in diameter (Fig. 3). Such a preferential growth along one of the crystallographic directions is explained by the anisotropic structure of  $\text{ZnWO}_4$ .

X-ray luminescence spectra investigation of the obtained powders showed the presence of a band with  $\lambda_{\text{max}} \approx 500$  nm. This band is typical for  $\text{ZnWO}_4$  single crystals and is caused by the emission of self-trapped excitons in the  $\text{WO}_6^{6-}$  oxyanion complex [16]. Fig. 3 illustrates the dependence of X-ray luminescence intensity on the morphology (sizes) of nanopowders synthesized at different conditions. Emission intensity of the “grains” is nearly zero (curve 1), while for “rods” the luminescence intensity (curve 3) is typically high for  $\text{ZnWO}_4$ . Similar dependences were observed in nanocrystals of different oxygen-containing compounds [17–19].

Such a big difference between curve 1 and curve 3 could be explained by the fact that the decreasing of nanocrystal sizes leads to an increase in oxygen vacancies, which in turn causes the formation of  $\text{WO}_6$  octahedra with distorted structure (luminescence centers with low probability of photon emission) [20]. It was shown that red luminescence is associated with the distorted complexes. The photoluminescence spectra of nano-sized  $\text{ZnWO}_4$  samples excited by irradiation with a wavelength of  $\lambda_{\text{ex}} = 355$  nm contain a red emission band at 700 nm (Fig. 4). The intensity of the red band increases with the decrease of the  $\text{ZnWO}_4$  nano-

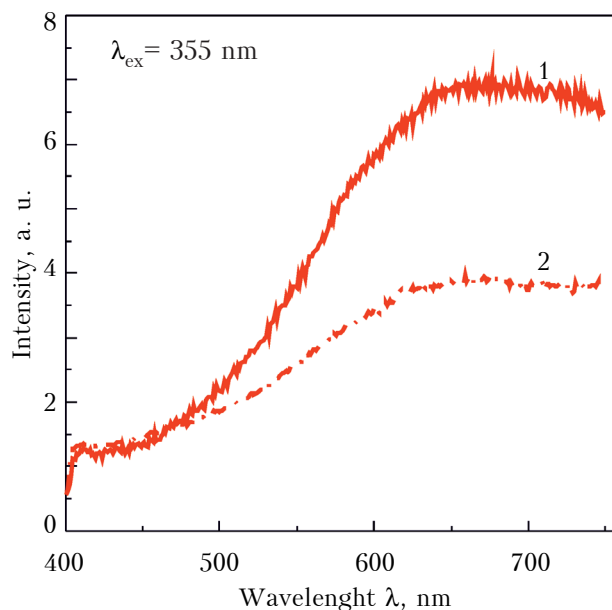


Fig. 4. Photoluminescence spectra of  $\text{ZnWO}_4$  “grains” before (1) and after annealing in air (2)

crystals size. At the same time the intensity of the red band for the samples annealed in air decreases, which indicates the healing of oxygen vacancies and decrease in concentration of distorted  $\text{WO}_6$  octahedra.

As it was shown in [20], that annealing of  $\text{ZnWO}_4$  nanopowders in air leads to a significant increase in X-ray luminescence intensity of the “grains” and has virtually no effect on intensity of the “rods” (Fig. 5).

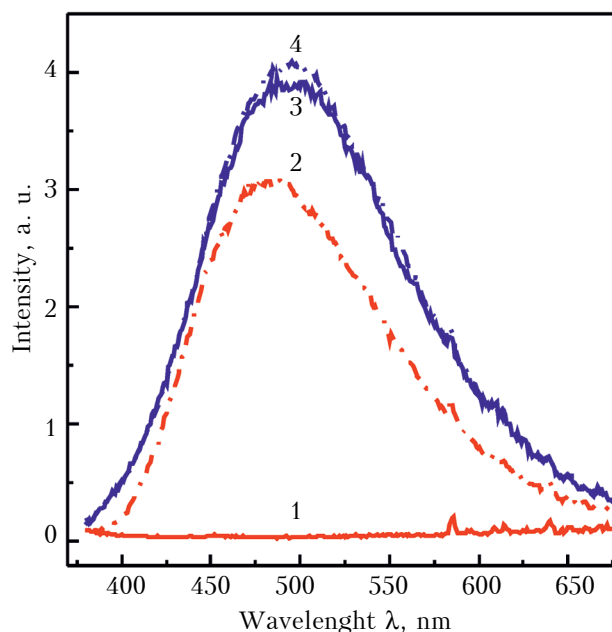


Fig. 5. X-ray luminescence spectra of  $\text{ZnWO}_4$  nanopowders:

1 – “grains”; 2 – “grains” after annealing; 3 – “rods”; 4 – “rods” after annealing



Under X-ray excitation, the red luminescence is absent even in the samples with high oxygen vacancy concentration. A competing nonradiative relaxation channel is formed in  $WO_6$  octahedra before air annealing, which causes a decrease in the luminescence intensity of the main emission band. After air annealing, the concentration of the distorted  $WO_6$  octahedra decreases, simultaneously increasing the main band intensity. This could possibly explain the increase in the intensity of the main band in X-ray luminescence spectrum after annealing the samples in air.

Composite samples with sizes of 10 × 10 × 2 mm were based on the obtained  $ZnWO_4$  nanopowders. The light outputs of the composite samples were measured with reference to the  $ZnWO_4$  single crystal (10 × 10 × 2 mm). The results of the measurements are shown in Table 1 (ZWO-25g contained “grains” of 25 nm, ZWO-100r – “rods” of 100 nm in length, ZWO-200r – “rods” of 200 nm in length).

The data in Table 1 show an increase of light output with the increase in nanoparticles size. However, the light output of the nanodispersed samples does not exceed 30% of that of the single crystal sample. Thus, this method does not ensure obtaining a scintillation material of the required quality.

*Flexible composite scintillators based on  $ZnWO_4$  obtained by molten salt synthesis*

Synthesizing nanomaterials using a low-temperature solvent offers the following advantages: the simplicity of the required equipment and a high efficiency of the particles obtained at temperatures below the melting point of the synthesized substance [21].

Single-phase nanocrystalline samples of the  $ZnWO_4$  scintillator were obtained by molten salt method (MSM) using a low-temperature  $LiNO_3$  solvent at 270°C for 6 and 16 hours [22]. The original sample was amorphous  $ZnWO_4$  obtained by co-precipitation method. Then, the precipitate

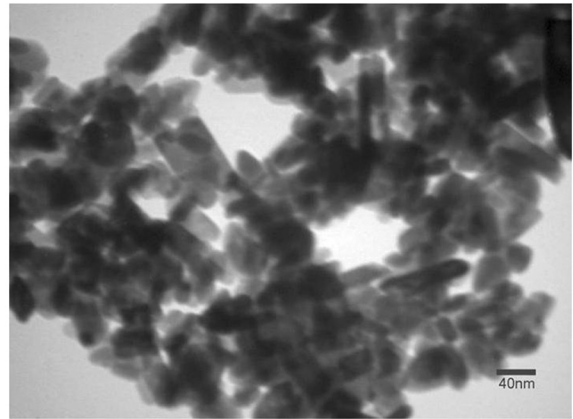


Fig. 6. TEM image of the nanopowder obtained by molten salt synthesis at the following conditions:  $ZnWO_4/LiNO_3$  ratio of 1:10 after annealing for 16 hours

was mixed with lithium nitrate in a ratio of 1:6 and 1:10.

The investigation of powder morphology using TEM showed that the largest granules (100 nm) were synthesized at  $ZnWO_4/LiNO_3$  ratio of 1:10 after synthesizing (annealing) for 16 hours (Fig. 6). The size of nanocrystals obtained at other synthesis conditions was less than 100 nm.

Table 2 shows the XRD data and calculated on their basis unit cell parameters of  $ZnWO_4$  nanocrystals obtained under different synthesis conditions (different  $ZnWO_4/LiNO_3$  ratios and different synthesis time periods). The crystal lattice of nanocrystals is markedly distorted in comparison with the ICDD database data for zinc tungstate  $ZnWO_4$  (JCDPS No 15-0774 [15]). This is particularly noticeable in the changing of the unit cell volume. There is a tendency for crystal lattice distortion to reduce (in particular, the lattice volume parameter  $V$ ) with the increase of the synthesis time at the same lithium nitrate concentration. The similar influence of synthesis conditions on the crystal lattice parameters was reported in [23].

Table 2

*Unit cell parameters of  $ZnWO_4$  nanocrystals obtained under different synthesis conditions, compared to the data for zinc tungstate presented in [15]*

Ratio $ZnWO_4:LiNO_3$ / time	$a, \text{Å}$	$b, \text{Å}$	$c, \text{Å}$	$\beta, ^\circ$	$V, \text{Å}^3$
1:6 / 6 h	4.68266(9)	5.75328(12)	4.94864(8)	90.6305(11)	133.311(4)
1:10 / 6 h	4.68258(9)	5.75424(12)	4.94881(8)	90.6352(12)	133.336(4)
1:6 / 16 h	4.68341(8)	5.74941(11)	4.94598(88)	90.6362(10)	133.171(4)
1:10 / 16 h	4.68340(9)	5.74908(11)	4.94544(8)	90.6386(10)	133.149(4)
$ZnWO_4$ [15]	4.69264	5.71546	4.92691	90.627	132.135

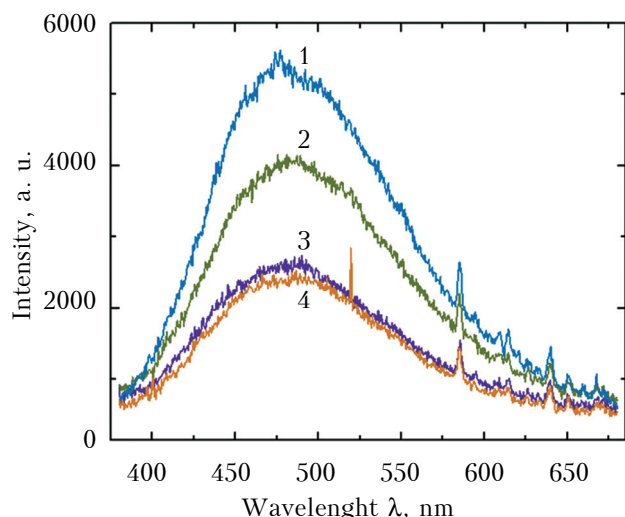


Fig. 7. The X-ray luminescence spectra of nanopowders obtained by molten salt synthesis under difference conditions (ratio  $ZnWO_4:LiNO_3$ , synthesis time): 1 – 1:10, 16 h; 2 – 1:6, 16 h; 3 – 1:6, 6 h; 4 – 1:10, 6 h

The X-ray luminescence spectra of the obtained powders show that nanosized crystal samples with less distorted crystal lattices demonstrate better scintillation performance. The highest luminescence intensity was demonstrated by the sample synthesized at the following conditions:  $ZnWO_4/LiNO_3$  ratio of 1:10 after annealing for 16 hours (Fig. 7). X-ray luminescence intensity of the obtained powders decreases with reduction in annealing time and concentration of low-temperature solvent.

The light output under X-ray excitation and the afterglow level of composite scintillator based on the  $ZnWO_4$  powder obtained by the molten salt method ( $ZnWO_4/LiNO_3 = 1:10$ , 16 h) are shown in Table 1 (ZWO-MSM) and Table 3, respectively.

The light output of the ZWO-MSM sample was 67% of that of the  $ZnWO_4$  single crystal (see Table 1). However, the afterglow level of ZWO-MSM is almost 2 times lower in the time range of 3–5 ms than that of the ZWO-30-250 $\mu$ m, which is very important for using these scintillators in computer tomography.

The afterglow level of  $ZnWO_4$  composite scintillators under X-ray excitation

Sample	Granule sizes	Afterglow level, %, after different periods of time			
		3 ms	5 ms	10 ms	20 ms
Polished $ZnWO_4$ single crystal	—	0.19	0.11	0.13	0.07
ZWO-30-250 $\mu$ m	250 $\mu$ m	0.14	0.103	0.068	0.045
ZWO-MSM	100 nm	0.072	0.064	0.055	0.047

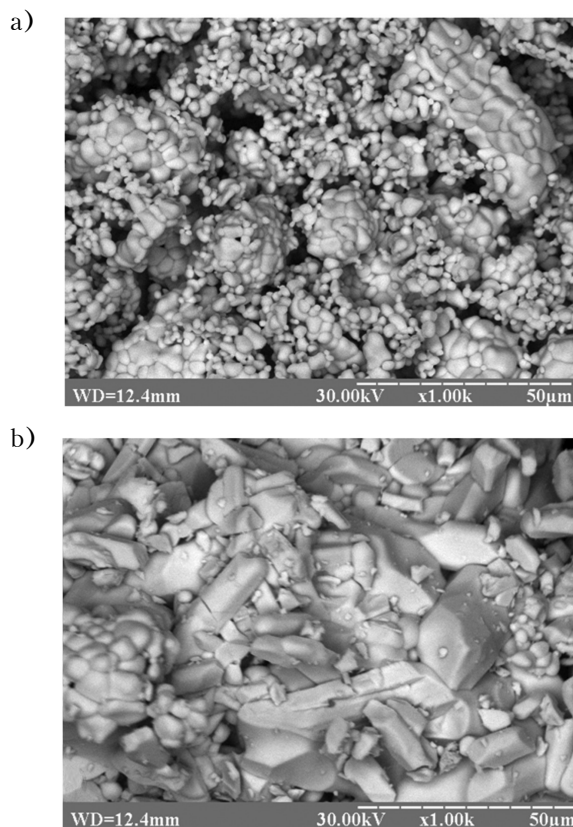


Fig. 8. SEM images of  $ZnWO_4$  crystallites synthesized at 950°C for 50 hours without a mineralizer (a) and with  $LiNO_3$  (b)

The improvement of the afterglow level of the scintillators can be explained by the entry of lithium ions from the solvent into the  $ZnWO_4$  crystal lattice, thus compensating the uncontrolled impurities charge (in particular, trivalent metal ions). This leads to changes in the defect structure and, as a result, to disappearing of deep charge traps. A similar effect of the lithium impurities on the afterglow was observed for cadmium tungstate crystals [24].

*Flexible composite scintillators based on  $ZnWO_4$  obtained by solid-state synthesis*

The most commonly used method for preparing of micro-sized oxide powders is solid-state synthesis (SSS), which is quite simple in technical realization. The use of a low-melting salt as a mineralizer (up to 10 wt. %) is one of the ways to accelerate solid-state reactions. The mineralizer reduces synthesis temperature, forms a melt, improves the diffusion of reagents and accelerates the growth of grains [25, 26].

As can be seen in the SEM images in Fig. 8, after 50 h long synthesis without

Table 3

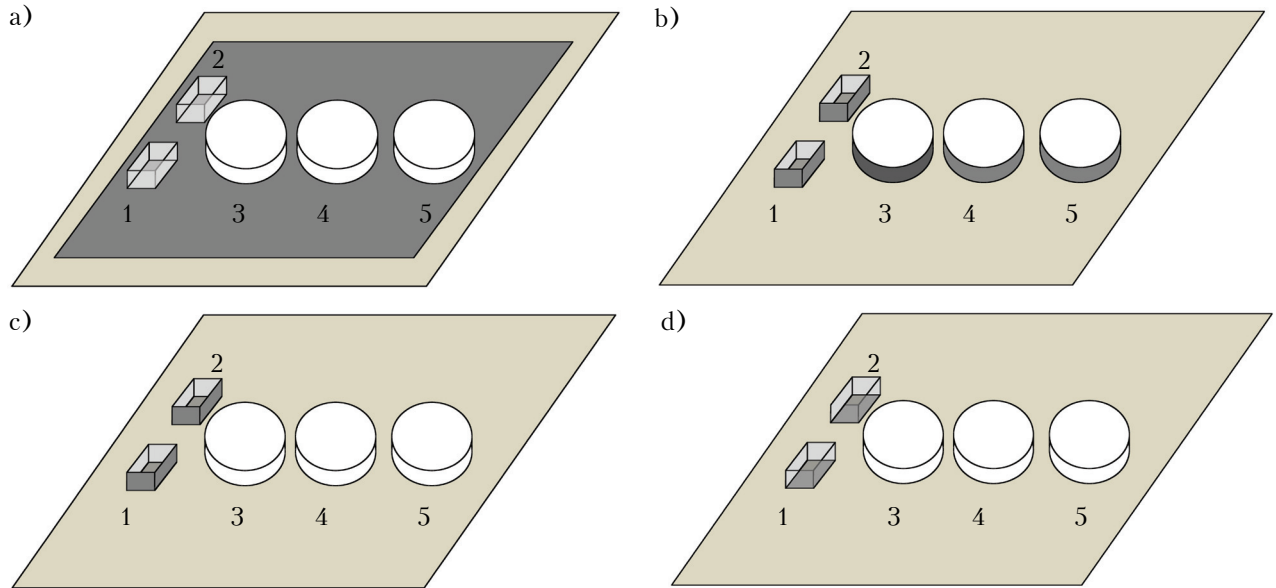


Fig. 9. The location scheme of samples on an objective table when measuring light output under X-ray excitation: *a* – all samples are placed on a white diffusion reflector; *b* – all sides of the samples, except the top, are covered with a white diffusion reflector; *c* – only the crystals are covered with a white diffusion reflector (all sides except the top); *d* – only the crystals are covered with a white diffusion reflector (bottom side only)  
 1 –  $ZnWO_4$  single crystal (10 10 2 mm); 2 –  $CdWO_4$  single crystal (10 10 2 mm); 3 – ZWO-30-250 $\mu m$ ; 4 – ZWO-SSS; 5 – ZWO-SSS- $LiNO_3$

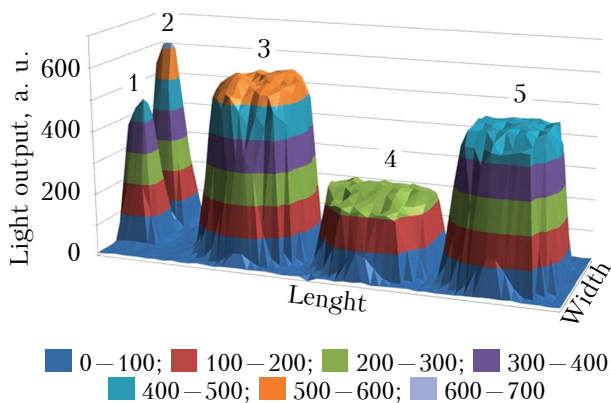


Fig. 10. Light output area distribution of different samples:

1 – single crystal  $ZnWO_4$ ; 2 – single crystal  $CdWO_4$ ; 3 – ZWO-30-250 $\mu m$ ; 4 – ZWO-SSS; 5 – ZWO-SSS- $LiNO_3$

the mineralizer, the sizes of the obtained  $ZnWO_4$  grains were 0.5–2  $\mu m$ , while after the synthesis under the same conditions but with the addition of lithium nitrate the sizes were 20–30  $\mu m$ .

Fig. 9 shows the samples location on the objective table when measuring the light output under X-ray excitation. For clarity, the white diffuse reflector is shown in dark gray. The light output of the composite samples (estimated under X-ray excitation using the optical transmission scheme shown in Fig. 1) is presented in Fig. 10 and Table 4. The samples were placed on the objective table and the light output throughout the scintillation sample was measured at 3 mm step. The light output of the sample was determined as the average value over the entire area.

Table 4

The light output under X-ray excitation of scintillation samples under different light collection conditions

Light output collection conditions	Light output, %				
	$CdWO_4$ single crystal	$ZnWO_4$ single crystal	ZWO-30-250 $\mu m$	ZWO-SSS	ZWO-SSS- $LiNO_3$
All samples placed on white diffusion reflector	288	100	280	155	272
All the sides of the samples except the top were covered by white diffusion reflector	130	100	121	60	107
Only the crystals were covered by a white diffusion reflector (all sides except top side)	133	100	84	51	80
Only the crystals were covered by a white diffusion reflector (just the bottom side)	136	100	88	54	83



As can be seen from Table 1, the light output of the composite sample based on the powder prepared by solid state synthesis with addition of the mineralizer (ZWO-SSS-LiNO<sub>3</sub>) is twice as high as that of the sample synthesized without the mineralizer (ZWO-SSS).

Table 4 shows that the light output of composite samples significantly depends on the light collection conditions. The light output of ZWO-SSS-LiNO<sub>3</sub> is comparable with the light output of the composite based on a crushed ZnWO<sub>4</sub> crystal and is close to a 10 × 10 × 2 mm CdWO<sub>4</sub> single crystal for all samples placed on a white diffusion reflector. In the case when the single crystals were covered with a white diffusion reflector, the light collection in single crystal samples improved, and the light output of ZWO-30-250 μm and ZWO-SSS-LiNO<sub>3</sub> is comparable to the ZnWO<sub>4</sub> single crystal. Also, in comparison with the single crystal, the composite scintillators demonstrate a good uniformity of scintillation parameters through the area of the sample. The results demonstrated in Fig. 10 were measured using the same light collection conditions for crystals and composite scintillators (all the sides of the samples except the top ones were covered by white diffusion reflector, see Fig. 9, b).

As was shown above, a significant increase in the light output of the composite scintillators made from crushed single crystals may be caused by better light collection conditions, which is obviously characteristic of ZWO-SSS-LiNO<sub>3</sub> composites as well.

### Conclusions

Research of the scintillation and luminescence characteristics of flexible composite scintillators made of micro- and nano-sized ZnWO<sub>4</sub> powders obtained by different methods showed the following.

The light output of the composite made of the ZnWO<sub>4</sub> powder obtained by grinding a ZnWO<sub>4</sub> bulk crystal is 84–280% of that of the ZnWO<sub>4</sub> single crystal and depends on the light collection conditions. Such a scintillator can be used in various X-ray and gamma-ray detectors. Composite samples of nano-sized ZnWO<sub>4</sub> powders obtained by the hydrothermal-microwave and molten salt methods are inferior to crushed crystal composite in terms of their scintillation characteristics.

The solid-state synthesis method using the lithium nitrate mineralizer makes it possible to obtain a ZnWO<sub>4</sub> micron powder with high scintillation characteristics, bypassing the single crystal growth stage. Under certain conditions of light collection, the parameters of a composite scintillator prepared from such a powder are comparable to those of a single crystal. Such composite scintillator can be

an alternative to a composite made of a powder obtained by grinding crystal.

Moreover, the manufactured flexible composite scintillators have a high uniformity of light output through the area, which makes them promising for digital radiography.

### REFERENCES

1. Buchele P., Richter M., Tedde S.A. et al. X-ray imaging with scintillator-sensitized hybrid organic photodetectors. *Nature Photonics*, 2015, no. 9, pp. 846–848. <http://dx.doi.org/10.1038/nphoton.2015.216>
2. Amouzegar Z., Naghizadeh R., Rezaie H.R. et al. Microwave engineering of ZnWO<sub>4</sub> nanostructures: Towards morphologically favorable structures for photocatalytic activity. *Ceramics International*, 2015, no. 41, pp. 8352–8359. <http://doi.org/10.1016/j.ceramint.2015.03.020>
3. Hojamberdiev M., Zhub G., Xua Y. Template-free synthesis of ZnWO<sub>4</sub> powders via hydrothermal process in a wide pH range. *Materials Research Bulletin*, 2010, no. 45, pp. 1934–1940. <http://doi.org/10.1016/j.materresbull.2010.08.015>
4. Wang Y., Liping L., Li G. Solvothermal synthesis, characterization and photocatalytic performance of Zn-rich ZnWO<sub>4</sub> nanocrystals. *Applied Surface Science*, 2017, no. 393, pp. 159–167. <http://doi.org/10.1016/j.apsusc.2016.10.001>
5. Klassen N.V., Kurlov V.N., Rossolenko S.N. et al. Scintillation fibers and nanoscintillators for improvement the spatial, spectrometric and time resolution of radiation detectors. *Bulletin of the Russian Academy of Sciences: Physics*, 2009, no. 73, pp. 1451–1456.
6. Reithmaier J.P., Søk G., Löffler A. et al. Strong coupling in a single quantum dot—semiconductor microcavity system. *Nature*, 2004, no. 432, pp. 197–200. <http://doi.org/10.1038/nature02969>
7. Zhmurin P.N., Malyukin Yu.V. *Spectroscopy of the rare-earth ions in the bulk and nanoscale crystals*. Kharkiv, Institute for single crystal, 2007, 160 p.
8. Nagornaya L.L., Grinyov B.V., Dubovik A.M. et al. Large volume ZnWO<sub>4</sub> crystal scintillators with excellent energy resolution and low background. *IEEE Trans. Nucl. Sci.*, 2009, no. 56, pp. 994–1001.
9. Rodriguez-Carvajal J., Roisnel T. FullProf.98 and WinPLOTR: New Windows95/NT applications for diffraction. *Commission for Powder Diffraction, International Union of Crystallography*, Newsletter no. 20, 1998
10. Nagornaya L., Onyshchenko G., Pirogov E. et al. Production of the high-quality CdWO<sub>4</sub> single crystals for application in CT and radiometric monitoring. *Nuclear Instruments and Methods in Physics Research. Section A*, 2005, no. 537, pp. 163–165. <https://doi.org/10.1016/j.nima.2004.07.258>
11. Lisitsyn V.M., Valiev D.T., Tupitsyna I.A. et al. Effect of particle size and morphology on the properties of luminescence in ZnWO<sub>4</sub>. *Journal of Luminescence*, 2014, no. 153, pp. 130–136. <http://doi.org/10.1016/j.jlumin.2014.03.024>
12. Ryzhikov V.D., Grinyov B.V., Boyarintsev A.Yu. et al. Multi-layered composite detectors for neutron detection. *Functional Materials*, 2018, no. 1, pp. 172–179. <https://doi.org/10.15407/fm25.01.172>
13. Liao H.W., Wang Y.F., Lui X.M. et al. Hydrothermal preparation and characterization of luminescent CdWO<sub>4</sub> nanorods. *Chemistry of Materials*, 2000, no. 12, pp. 2819–2821. <http://doi.org/10.1021/cm000096w>
14. Yakubovskaya A.G., Tupitsina I., Sofronov D. et al. Microwave hydrothermal synthesis and luminescent properties



of ZnWO<sub>4</sub> nanoparticles. *Functional Materials*, 2013, no. 20, pp. 523–527. <http://dx.doi.org/10.15407/fm20.04.523>

15. JCDPS PDF-1 File, *International Committee for Diffraction Data*, PA, USA, 1994.

16. Nagirnyi V., Feldbach E., Jonsson L. et al. Energy transfer in ZnWO<sub>4</sub> and CdWO<sub>4</sub> scintillators. *Nuclear Instruments and Methods in Physics Research. Section A*, 2002, no. 486, pp. 395–398. [http://doi.org/10.1016/S0168-9002\(02\)00740-4](http://doi.org/10.1016/S0168-9002(02)00740-4)

17. Krutyak N., Mikhaïlik V., Vasil'ev A. et al. The features of energy transfer to the emission centers in ZnWO<sub>4</sub> and ZnWO<sub>4</sub>:Mo. *Journal of Luminescence*, 2013, no. 144, pp. 105–111. <http://10.1016/j.jlumin.2013.06.039>

18. Vistovskyy V., Chornodolskyy Ya., Gloskovskii A. et al. Modeling of X-ray excited luminescence intensity dependence on the nanoparticle size. *Radiation Measurements*, 2016, vol. 90, pp. 174–177. <https://doi.org/10.1016/j.radmeas.2015.12.010>

19. Wang Y., Ma J., Tao J. et al. Hydrothermal synthesis and characterization of CdWO<sub>4</sub> nanorods. *Journal of the American Ceramic Society*, 2006, vol. 89, iss. 9, pp. 2980–2982. <https://doi.org/10.1111/j.1551-2916.2006.01171.x>

20. Tupitsyna I.A., Maksimchuk P.O., Yakubovskaya A.G. et al. X-ray and photo-excited luminescence of ZnWO<sub>4</sub> nanoparticles with different size and morphology. *Functional Materials*, 2016, no. 23, pp. 535–539. <http://doi.org/10.15407/fm23.04.357>

21. Jan B., Lei F. Molten salt synthesis, characterization and luminescence of ZnWO<sub>4</sub>:Eu<sup>3+</sup> nanophosphors. *Journal of Alloys and Compounds*, 2010, vol. 507, iss. 2, pp. 460–465. <http://doi.org/10.1016/j.jallcom.2010.07.203>

22. Yakubovskaya A.G., Katrunov K.A., Tupitsina I.A. et al. Nanocrystalline zinc and cadmium tungstates: Morphology, luminescent and scintillation properties. *Functional Materials*, 2011, no. 18, pp. 446–451.

23. Chen L., Fleming P., Morris V. et al. Size-related lattice parameter changes and surface defects in ceria nanocrystals. *The Journal of Physical Chemistry C*, 2010, no. 114, pp. 12909–12919. <http://doi.org/10.1021/jp1031465>

24. Vedda A., Moretti F., Fasoli M. et al. Intrinsic trapping and recombination centers in CdWO<sub>4</sub> investigated using thermally stimulated luminescence. *Physical Review B*, 2009, vol. 80, iss. 4, pp. 045104-1-7. <https://doi.org/10.1103/PhysRevB.80.045104>

25. Gorshkov V.S., Saveliev V.G., Fedorov N.F. *Fizicheskaya Khimiya Silikatov i Drugikh Tugoplavkikh Soedinenii* [Physical Chemistry of Silicates and Other Refractory Compounds]. Moscow, Vysshaya shkola, 1988, 203 p. (Rus)

26. Budnikov P.P., Gistling A.M. *Reaktsii v Smesyakh Tverdykh Veshchestv* [Reactions in Mixtures of Solid Substances], Moscow, Stroiizdat, 1971, 311 p. (Rus)

Received 21.05 2018

DOI: 10.15222/ТКЕА2019.1-2.40

УДК 539.1.074.3 : 62-492.2 : 546.47'78'21

V. С. ТИЊКОВА, Г. Г. ЯКУБОВСЬКА<sup>1</sup>,  
І. А. ТУПЦІНА<sup>1</sup>, С. Л. АБАШИН<sup>2</sup>,  
Г. Н. ПУЗАН<sup>3</sup>, С. О. ТРЕТЬЯК<sup>1</sup>

Україна, м. Харків,

<sup>1</sup>Інститут сцинтиляційних матеріалів НАН України;

<sup>2</sup>Національний аерокосмічний університет  
«Харківський авіаційний інститут»;

<sup>3</sup>НТК «Інститут монокристалів» НАН України

E-mail: zvereva@isma.kharkov.ua

## ГНУЧКІ КОМПОЗИЦІЙНІ СЦИНТИЛЯТОРИ НА ОСНОВІ МІКРО- ТА НАНОПОРОШКІВ ZnWO<sub>4</sub>

Для отримання матеріалів, придатних для використання в сучасних сцинтиляційних детекторах (для неруйнівного контролю, цифрової радіографії і рентгенографії, α-, β-, γ- та нейтронної реєстрації), ведуться пошуки ефективних технологічних методів. Одним з перспективних напрямків досліджень в цій області є створення композиційних сцинтиляторів на основі мікро- і нанорозмірних кристалічних порошків. Властивості таких сцинтиляційних порошків істотно залежать від розміру складових їхніх частинок і морфології, отже, керуючи цими параметрами, можна створити сцинтиляційні детектори з високими сцинтиляційними характеристиками.

Вольфрамат цинку (ZnWO<sub>4</sub>) – це перспективний матеріал, який завдяки унікальній комбінації властивостей може стати успішною заміною CdWO<sub>4</sub>, що містить токсичний кадмій. У даній роботі проведені дослідження, спрямовані на пошук ефективного способу отримання порошку ZnWO<sub>4</sub> для розробки гнучких композиційних сцинтиляторів з високими функціональними характеристиками, такими як світловий вихід і рівень післясвітіння.

Досліджували порошки вольфрамату цинку (ZnWO<sub>4</sub>), синтезовані трьома способами: гідротермальним з мікрохвильовим нагрівом, розчин-розплавним методом і методом твердофазового синтезу. Отримані нано- та мікропорошки слугували наповнювачем для створення гнучких композиційних сцинтиляторів. Як сполучне був використаний силіконовий каучук. Морфологію зразків вивчали за допомогою трансмісійної та скануючої електронної мікроскопії. Досліджено люмінесцентні характеристики і сцинтиляційні параметри отриманих композитів. Продемонстровано залежність сцинтиляційних параметрів композитів від морфологічних особливостей нано- та мікрокристалітів ZnWO<sub>4</sub>.

Світловий вихід композиту з порошку, виготовленого з подрібненого об'ємного кристалу ZnWO<sub>4</sub>, становить 84–280% від світлового виходу монокристалла ZnWO<sub>4</sub> і залежить від умов збору світла.

Композиційні зразки з нанорозмірних порошків  $ZnWO_4$ , отриманих гідротермально-мікрохвильовим і розчин-розплавним методами, за своїми сцинтиляційними характеристиками поступаються компози- ту з подрібненого кристала. Твердофазовий метод синтезу з використанням мінералізатора на основі нітрату літію дозволяє отримувати мікронний порошок  $ZnWO_4$  з високим значенням світлового виходу, минаючи стадію вирощування монокристалу. Параметри композитів на основі такого порошку близькі до параметрів монокристала вольфрамату кадмію.

Ключові слова: вольфрамат цинку, нанорозмірні кристали, мікророзмірні кристали, композиційні сцинтилятори, світловий вихід, рівень післясвітіння.

V. S. ТИНЬКОВА<sup>1</sup>, А. Г. ЯКУБОВСКАЯ<sup>1</sup>, И. А. ТУПИЦЫНА<sup>1</sup>,  
С. Л. АБАШИН<sup>2</sup>, А. Н. ПУЗАН<sup>3</sup>, С. Е. ТРЕТЬЯК<sup>1</sup>

Украина, г. Харьков, <sup>1</sup>Институт сцинтилляционных материалов НАН Украины;

<sup>2</sup>Национальный аэрокосмический университет

«Харьковский авиационный институт»;

<sup>3</sup>НТК «Институт монокристаллов» НАН Украины

E-mail: zvereva@isma.kharkov.ua

## ГИБКИЕ КОМПОЗИЦИОННЫЕ СЦИНТИЛЛЯТОРЫ НА ОСНОВЕ МИКРО- И НАНОПОРОШКОВ $ZnWO_4$

Для получения материалов, пригодных для использования в современных сцинтилляционных детекторах (для неразрушающего контроля, цифровой радиографии и рентгенографии,  $\alpha$ -,  $\beta$ -,  $\gamma$  и нейтронной регистрации), ведутся поиски эффективных технологических методов. Одним из перспективных направлений исследований в этой области является создание композиционных сцинтилляторов на основе микро- и наноразмерных кристаллических порошков. Свойства таких сцинтилляционных порошков существенно зависят от размера составляющих их частиц и морфологии, а значит, управляя этими параметрами, можно создать сцинтилляционные детекторы с высокими функциональными характеристиками.

Вольфрамат цинка ( $ZnWO_4$ ) — это перспективный материал, который благодаря уникальной комбинации свойств может быть успешной заменой  $CdWO_4$ , содержащего токсичный кадмий. В настоящей работе проведены исследования, направленные на поиск эффективного способа получения порошка  $ZnWO_4$  для разработки гибких композиционных сцинтилляторов с высокими функциональными характеристиками, такими как световой выход и уровень послесвечения.

Исследовали порошки вольфрамата цинка ( $ZnWO_4$ ), синтезированные тремя способами: гидротермальным с микроволновым нагревом, раствор-расплавным методом и методом твердофазного синтеза. Полученные нано- и микропорошки служили наполнителем для создания гибких композиционных сцинтилляторов. В качестве связующего был использован силиконовый каучук. Морфологию образцов изучали с помощью трансмиссионной и сканирующей электронной микроскопии. Исследованы люминесцентные характеристики и сцинтилляционные параметры полученных композитов. Продемонстрирована зависимость сцинтилляционных параметров композитов от морфологических особенностей нано- и микрокристаллитов  $ZnWO_4$ .

Световой выход композита из порошка, приготовленного из измельченного объемного кристалла  $ZnWO_4$ , составляет 84–280% от светового выхода монокристалла  $ZnWO_4$  и зависит от условий светособирания. Композиционные образцы из наноразмерных порошков  $ZnWO_4$ , полученных гидротермально-микроволновым и раствор-расплавным методами, по своим сцинтилляционным характеристикам уступают композиту из измельченного кристалла. Твердофазный метод синтеза с использованием минерализатора на основе нитрата лития позволяет получить микронный порошок  $ZnWO_4$  с высоким значением светового выхода, минуя стадию выращивания монокристалла. Композиты на основе такого порошка обладают параметрами, близкими к параметрам монокристалла вольфрамата кадмия.

Ключевые слова: вольфрамат цинка, наноразмерные кристаллы, микро- и наноразмерные кристаллы, композиционные сцинтилляторы, световой выход, уровень послесвечения.

### Описание статьи для цитирования:

Tinkova V. S., Yakubovskaya A. G., Tupitsyna I. A., Abashin S. L., Puzan A. N., Tretyak S. O. Flexible composite scintillators based on  $ZnWO_4$  micro- and nanopowders. Технология и конструирование в электронной аппаратуре, 2019, № 1-2, с. 40–49. <http://dx.doi.org/10.15222/TKEA2019.1.40>

### Cite the article as:

Tinkova V. S., Yakubovskaya A. G., Tupitsyna I. A., Abashin S. L., Puzan A. N., Tretyak S. O. Flexible composite scintillators based on  $ZnWO_4$  micro- and nanopowders. Tekhnologiya i Konstruirovaniye v Elektronnoi Apparature, 2019, no. 1-2, pp. 40–49. <http://dx.doi.org/10.15222/TKEA2019.1.40>